Search for gravitational waves

Guido Pizzella
Universita' di Roma Tor Vergata, Italy
INFN, Laboratori Nazionali di Frascati, Italy

September 13, 2000

Abstract

The search for gravitational waves with cryogenic resonant detectors is reviewd and the results so far obtained are presented.

1 Gravitational waves in General Relativity

As well known gravitational waves (GW) were a prediction of General Relativity (GR) in 1916, although they were already foreseen in 1900 by Lorentz and in 1905 independently by Poincare, on the basis of the analogy of the Newtonian gravitational force with the Coulombian electrical force.

We recall [1] that the GR fundamental equation is

$$R_{ik} = \frac{8\pi G}{c^2}(T_{ik} - \frac{1}{2}g_{ik}T) \tag{1}$$

where R_{ik} is the Ricci tensor, T_{ik} if the energy-momentum tensor (T is the trace) and g_{ik} is the metric tensor which enters non-linearly in the expression of R_{ik}. The tensor g_{ik} is the unknown of the non-linear eq. 1 and it describes the action of gravity via the geometry of space-time.

In vacuum eq. 1 becomes

$$R_{ik} = 0 \tag{2}$$

This equation, being non linear, cannot be solved in general. However a simple solution is found (already by Einstein in 1916) if the hypothesis is

made of a weak gravitational field, that is

$$g_{ik} \simeq \delta_{ik} + h_{ik} \tag{3}$$

where δ_{ik} is the Kronecker symbol and $h_{ik} << 1$. In this case eq. 1 becomes linear and reduces to the wave equation,

$$\Box h_{ik} = 0 \tag{4}$$

in vacuum. Note the important result that the GW travel with the speed of light.

In general the symmetric tensor h_{ik} has ten components, but a convenient choice of the reference system and using the Lorentz gauge leave only two independent components, often indicated with h_+ and $h_\times$ corresponding to two wave polarizations.

For a plane wave travelling along the x-direction we can write

$$h_+ = A_+ e^{i(\omega t - kx)} \tag{5}$$

$$h_\times = A_\times e^{i(\omega t - kx)} \tag{6}$$

and the h_{ik} matrix has all null components but

$$h_{yy} = h_{zz} = h_+ \tag{7}$$

$$h_{yz} = h_{zy} = h_\times \tag{8}$$

2 Sources of gravitational waves

In presence of matter eq. 4 is written as

$$\Box h_{ik} = \frac{16G}{c^4} \tau_{ik} \tag{9}$$

where τ_{ik} is related to the tensor T_{ik}. The solution of this equation is mathematically identical to the solution for the electromagnetic waves (here we have a tensor instead than a vector) given with the so-called retarded potential

$$h_{ik} = -\int (\frac{\tau_{ik}}{r})_{t-\frac{r}{c}} dV \tag{10}$$

r being the distance of the source. The main difference with the electromagnetic case is that in the multipole expansion the dipole term is null for the GW. This is because the conservation laws (energy and momentum) in GR are expressed by

$$\frac{\partial \tau_{ik}}{\partial x_k} = 0 \tag{11}$$

(null divergence of τ_{ik}), and this is just the dipole term in the multipole expansion of eq. 10. Thus the first term is the quadrupole term, and this characterizes the GW emission.

It can be shown [1] that the quadrupole term generates a total irradiated power averaged on all directions given by

$$W = \frac{G}{45c^5}(\frac{d^3}{dt^3}D_{\alpha\beta})^2 \tag{12}$$

where we have the third time derivative of $D_{\alpha\beta}$ which is the mass quadrupole tensor

$$D_{\alpha\beta} = \int \rho(3x_\alpha x_\beta - \delta_{\alpha\beta}x_\gamma^2)dV \tag{13}$$

with obvious meaning for symbols (here α and β run from 1 to 3, only space coordinates).

Already Einstein in 1916 noted that the power irradiated by a source which one can imagine to realize in a laboratory is so small that
it has a practically vanishing value.

It is interesting to calculate such a value for a very large metallic bar rotating around the x axis perpendicular to its own axis and passing through its center-of-mass (say, an iron bar 2L=20 meter long and radius R=1 m square meter, M=500 tonne).

In the (y,z) plane, considering an unidimensional bar with mass density $\lambda = \frac{M}{2L}$, since

$$y = rcos\theta \qquad\qquad z = rsin\theta \tag{14}$$

we have

$$D_{yy} = \int_{-L}^{L} \lambda dr(2r^2cos^2\theta - r^2sin^2\theta) = \frac{ML^2}{3}(2cos^2\theta - sin^2\theta) \tag{15}$$

and

$$D_{zz} = \int_{-L}^{L} \lambda dr(2r^2sin^2\theta - r^2cos^2\theta) = \frac{ML^2}{3}(2sin^2\theta - cos^2\theta) \tag{16}$$

$$D_{xx} = \int_{-L}^{L} \lambda dr(-r^2) = -\frac{1}{3}ML^2 \tag{17}$$

$$D_{yz} = \int_{-L}^{L} \lambda dr(3yz) = ML^2 sin\theta cos\theta \tag{18}$$

$$D_{xy} = D_{xz} = 0 \tag{19}$$

Putting

$$\frac{1}{3}ML^2 = I \tag{20}$$

the moment of inertia with respect to the center of mass we calculate

$$\frac{d^3}{dt^3}D_{yy} = 12\omega^2 I sin2\theta \tag{21}$$

$$\frac{d^3}{dt^3}D_{zz} = -12\omega^2 I sin2\theta \tag{22}$$

$$\frac{d^3}{dt^3}D_{yz} = \frac{d^3}{dt^3}D_{yz} = -12\omega^2 I cos2\theta \tag{23}$$

We have

$$W = \frac{G}{45c^5}[(\frac{d^3}{dt^3}D_{xx})^2 + (\frac{d^3}{dt^3}D_{yy})^2 + (\frac{d^3}{dt^3}D_{zz})^2 + 2(\frac{d^3}{dt^3}D_{yz})^2] \tag{24}$$

$$W = \frac{G}{45c^5}144\omega^6 I^2(2sin^2 2\theta + 2cos^2 2\theta) = \frac{32G}{5c^5}I^2\omega^6 \tag{25}$$

Numerically we have a total irradiated power of GW

$$W = 2.2\ 10^{-29}\ watt \tag{26}$$

an extremely small quantity which cannot be detected with the present instrumentation.

2.1 Emission of GW by binary systems

The quantity $\frac{G}{c^5}I^2\omega^6$ of eq. 25 is typical for the emission of GW. In the case of a binary system, two stars (normal or collapsed stars) rotating one with respect to the other one, the emitted power is

$$W = \frac{32G}{5c^5}(\frac{m_1 m_2}{m_1 + m_2})^2 R^4 \Omega^6 \tag{27}$$

for circular orbits of radius R and with angular velocity Ω. It is interesting to note that for these systems in the framework of GR we *must* always have emission of GW.

A few years ago Hulse and Taylor studied the binary system PSR 1913+16 which include a pulsar and found, among many verifications of the GR theory, that the system was loosing energy at a rate of $\simeq 6.4\ 10^{23}\ watt$ in very good agreement with that calculated with eq. 27 and thus they concluded that the system was emitting GW. For this work Hulse and Taylor obtained the Nobel Prize.

2.2 CHIRP emission of GW

A binary system after a few thousand years looses all its rotational energy via emission of GW. Considering a system made by two collapsed objects, during the last few minutes before collision, the GW frequency varies in a way called $CHIRP$, it increases from a few hertz to the order of 1 kHz and the wave amplitude also increases in a very specific way.

From the wave amplitude and frequency it is possible to calculate the distance of the source and all properties of the binary system, in this way setting a new and absolute way to estimate the distances in the Universe.

2.3 Emission of GW by pulsars

If the pulsar is a perfect sphere there is no emission of GW, since the third time derivative of the quadrupole moment of inertia is null. However in the case the pulsar is not spherical, indicating with a and b two different equatorial radii we have the emission

$$W = \frac{32}{5}\frac{G}{c^5} I^2 \Omega^6 \frac{(a-b)^2}{ab} \tag{28}$$

As an example we have calculated the possible GW emission by the fast pulsar 1937+214, at a distance of 2.5 kpc, rotating with a period of 1.557806448 ms. If we assume that the observed energy loss of $2\ 10^{29}\ watt$ be due to emission of GW (which is a strong assumption) we find that the GW amplitude at the Earth is $h \sim 3\ 10^{-27}$, corresponding to a deviation from sphericity of $a - b = 100 \mu m$. We notice that for sources of this type the GW emission depends strongly on the astrophysical model.

2.4 Emission of GW by supernovae

Also in this case the GW emission depends strongly on the adopted model. If the gravitational collapse occurs with spherical symmetry no GW are emitted. However many astrophysicists believe that during the collapse the star breaks in many pieces and the spherical symmetry is not conserved. It is clear that the estimation of GW emission varies considerably form one model to an other one.

If we assume that at the end of the collapse a mass M_{gw} is entirely converted into GW, the following formula holds

$$h = \frac{1}{R\omega_{gw}}\sqrt{\frac{8GM_{gw}}{c\tau_{gw}}} = 3.1\ 10^{-20}\frac{10Mpc}{R}\sqrt{\frac{M_{gw}}{M_o}} \tag{29}$$

where τ_{gw} (conventionally taken equal to 1 ms) is the duration of the burst around the frequency ω_{gw}, at the distance R. According to the various astrophysical models the fraction of mass going into GW varies from zero up to about 1% of a solar mass.

2.5 Fall into a Schwarzschild black hole

It was worth to mention that GW are emitted if a body with mass m falls into a Schwarzschild black hole [5] with mass M_{bh}. It is calculated that a burst of GW is emitted with total energy

$$\triangle E = 0.0025\frac{m^2c^2}{M_{bh}} \tag{30}$$

with a frequency spectrum peaked at the frequency

$$f_{bh} = 4900\frac{M_o}{M_{bh}} \tag{31}$$

3 Interaction of a GW with free masses

As well known, in the GR theory it is always possible to choose a reference system that nullifies the gravitational field in a given point (think of the falling elevator). This makes it impossible to measure the properties of a gravitational field using only one test mass. We recall that the properties of

a gravitational field are expressed by the curvature tensor R_{iklm} of which the Ricci tensor R_{ik} is a contraction

$$R_{ik} = g^{lm} R_{limk} = R^{l}_{ilk} \tag{32}$$

Only if all components of the tensor R_{iklm} are zero we can state that there is no gravitational field. This is not true for the Ricci tensor, as shown by eq. 2 where $R_{ik} = 0$ but a non-null weak field solution exists.

Thus we need two test masses. The experimental problem consists in measuring the change of their mutual distance under the action of a gravitational field. The distance between them can be determined from the two geodesic lines written properly with the covariant derivative. It can be shown that for any vector u^i the following formula holds

$$u^{i}_{;kl} - u^{i}_{;lk} = -R^{i}_{mkl} u^{m} \tag{33}$$

where the symbol ; indicates the covariant derivative. From this formula, identifying the vector u^i with the four-velocity of one of the test masses we obtain the *geodesic deviation equation* written for the case of velocity much smaller than light and in absence of other forces but gravity

$$\frac{\partial^2 \eta^i}{\partial s^2} + \eta^k R^{i}_{0k0} = 0 \tag{34}$$

where η^i is the distance between the two test masses and s is the coordinate $ds = cd\tau$, with τ the proper time along the particle trajectory.

The eq. 34 is at the basis of all detectors for GW. From this equation, for the case of GW we obtain

$$\frac{\partial^2 \eta^i}{\partial t^2} = \eta^k \frac{\partial^2 h^{i}_{k}}{\partial t^2} \tag{35}$$

We apply now this equation to the case of two test masses along the y-axis at positions $\pm\frac{l}{2}$ with the GW travelling along the x-axis. We get

$$\ddot{\eta}^i = \ddot{\xi}^i = \frac{1}{2} \ddot{h}^{i}_{2} l \tag{36}$$

where we indicate with ξ^i the change in the distance η^i. Writing the four components we obtain for given initial conditions

$$\xi^o = 0, \qquad \xi^1 = 0, \qquad \xi^2 = \frac{l}{2} h_+, \qquad \xi^3 = \frac{l}{2} h_\times \tag{37}$$

More in general for a ring of test masses in the (y,z) plane with radius r, indicating with θ the angle of a diameter with the y-axis we have the following deformation of the ring

$$\xi^2 = r(h_+ cos\theta + h_\times sin\theta) \tag{38}$$

$$\xi^3 = r(h_\times cos\theta - h_+ sin\theta) \tag{39}$$

This formula clarifies the relative effect of the two different polarizations. We notice that the effect produced by the wave h_+ is identical to that produced by the wave $h_\times$ with a rotation by an angle of 45^o.

4 Interaction of a GW with an oscillator

A simple harmonic oscillator constituted by two masses at distance l connected by a spring with dissipation forces and subjected to a GW of amplitude h impinging perpendicularly to its axis obeys to the equation

$$\ddot{\xi} + 2\beta_1 \dot{\xi} + \omega_o^2 \xi = \frac{l}{2}\ddot{h} \tag{40}$$

where we have indicated with ξ the change in the distance l between the two masses and with $2\beta_1$ the dissipation forces per unit mass. In writing eq. 40 we have started from eq. 38 for $\theta = 0$, $h_\times = 0$ and we have put for simplicity $h_+ \equiv h$.

It is convenient to make use of the Fourier transforms. In our notations:

$$\xi(\omega) = \int_{-\infty}^{\infty} \xi(t) e^{-i\omega t} dt \tag{41}$$

$$\xi(t) = \frac{1}{2\pi} \int_{-\infty}^{\infty} \xi(\omega) e^{i\omega t} d\omega \tag{42}$$

A particular solution of eq. 40 is

$$\xi(\omega) = T_o(\omega) h(\omega) \tag{43}$$

where $h(\omega)$ is the Fourier transform of $h(t)$ and $T_o(\omega)$ is the *transfer function*

$$T_o(\omega) = \frac{l}{2} \frac{\omega^2}{(\omega^2 - \omega_0^2) - 2i\beta_1\omega} \tag{44}$$

The square modulus $|T_o(\omega)|^2$ of the transfer function gives all important information. For small dissipation we get the *quality factor* Q

$$Q = \frac{\omega_o}{2\beta_1} \tag{45}$$

For $Q >> 1$ the transfer function has two resonances at frequencies

$$\omega_{1,2} = i\beta_1 \pm \omega_o \tag{46}$$

and we can write the solution in the form

$$\xi(t) = \frac{1}{2\pi}\frac{l}{2}\int_{-\infty}^{\infty} \frac{\omega^2 H(\omega) e^{i\omega t}}{(\omega - \omega_1)(\omega - \omega_2)} d\omega \tag{47}$$

This can be transformed in

$$\xi(t) = \frac{1}{2\pi}\frac{l}{2}\int_{-\infty}^{\infty} \frac{(\omega - \omega_1)(\omega - \omega_2) - \omega_1\omega_2 + \omega(\omega_1 + \omega_2)}{(\omega - \omega_1)(\omega - \omega_2)} d\omega \tag{48}$$

Performing the integral and for the case $H(\omega_1) = H(\omega_2)$, which is a common case, we finally obtain

$$\xi(t) \simeq -\frac{l}{2} H(\omega_o) e^{-\beta_1 t} \omega_o \sin \omega_o t + \frac{l}{2} h(t) \tag{49}$$

4.1 GW modelled as a delta signal

In many real cases the GW can be modelled with a delta-function. This is for a gravitational collapse when one or several GW bursts are expected, each burst lasting a small fraction of a second or also for the very final stage of a coalescence binary system when the two stars collide. In this case the Fourier spectrum of $h(t)$ is flat and we can apply eq. 49[1].

$$\xi(t) = -\frac{l}{2} e^{-\beta_1 t} h(\omega_o) \omega_o sin \omega_o t \tag{50}$$

[1]Neglecting the transient delta-term.

4.2 GW modelled as monochromatic wave

In this case, which we expect for GW emitted by pulsars, we have

$$h(\omega) = \pi h_o[\delta(\omega - \Omega) + \delta(\omega + \Omega)] \tag{51}$$

where Ω is the frequency of the GW. In the case $\Omega = \omega$, substituting in eq. 47 and using 45 we get

$$\xi(t) = -\frac{l}{2} h_o Q sin\omega t \tag{52}$$

5 Interaction of GW with a metallic cylinder

The resonant GW detectors in operation today are of cylindrical shape and made of Aluminium or Niobium. Let us then study [2, 3] the interaction of a GW with a metallic cylinder of mass M and length L with its axis in the direction of the z-coordinate.

We split the cylinder in slashes of thickness dz, each slash delimitate by two sections with coordinates z and $z + dz$. Each section vibrates around its equilibrium position with displacement $\xi(z, t)$ depending on time on position. We shall consider the following quantities used in the theory of elasticity: The *strain*

$$u = \frac{\partial \xi}{\partial z} \tag{53}$$

and the stress

$$\sigma = Yu + D\frac{\partial u}{\partial t} \tag{54}$$

Y is the Young modulus and D expresses the losses.

We write now the Newton law for the slash of thickness dz and mass $dm = \rho S dz$, where S is the cylinder section:

$$\rho\frac{\partial^2 \xi}{\partial t^2} = \frac{\partial \sigma}{\partial z} + F_g \tag{55}$$

where F_g is the force per unit volume due to the GW.

For estimating this force we reason in the following way. Let us consider two slashes of thickness dz, one located at z and the other one at $-z$. Under

the action of the GW alone the distance between the two slashes changes according to eq. 36, just like under the action of a force per unit volume

$$\rho\ddot{\xi} = \rho z\ddot{h} \tag{56}$$

We choose our reference system in such a way that gravity is zero at the origin. We can consider the motion of one of the two slashes with respect to the origin as subjected to a force which is one half of that acting between the two slashes, thus we get

$$F_g = \frac{\rho z}{2}\ddot{h} \tag{57}$$

Putting this in eq. 55 we obtain the equation

$$\rho\ddot{\xi} - Y\frac{\partial^2\xi}{\partial z^2} - D\frac{\partial}{\partial t}\frac{\partial^2\xi}{\partial z^2} = \frac{\rho z}{2}\ddot{h} \tag{58}$$

Using the Fourier transforms $\xi(\omega, z)$ we obtain

$$\frac{d^2\xi(\omega,z)}{dz^2}(Y + i\omega D) + \omega^2\rho\xi = \frac{\rho z}{2}\omega^2 h(\omega) \tag{59}$$

The general solution is

$$\xi(\omega, z) = \xi_1(\omega)e^{i\alpha z} + \xi_2(\omega)e^{-i\alpha z} + \frac{z}{2}h(\omega) \tag{60}$$

with

$$\alpha_{1,2} = \pm i\sqrt{\frac{\omega^2\rho}{Y}}(1 - \frac{i}{2Q}) = \pm i\alpha \tag{61}$$

where

$$Q = \frac{Y}{\omega D} \tag{62}$$

We now impose the boundary conditions, the displacement is zero at the origin $\xi(0,\omega) = 0$ and the stress at the bar ends must be zero $(\frac{\partial\xi}{\partial z})_{\pm\frac{L}{2}} = 0$. We finally obtain the solution

$$\xi(\omega, z) = \frac{h(\omega)}{2}(\frac{z}{2} - \frac{sin\alpha z}{2\alpha cos\frac{\alpha L}{2}}) \tag{63}$$

We notice that there are resonances. This is when

$$cos\frac{\alpha L}{2} \simeq 0 \tag{64}$$

Introducing the sound velocity in the bar material

$$v = \sqrt{\frac{Y}{\rho}} \tag{65}$$

and neglecting the losses ($Q >> 1$) the denominator is zero when

$$\alpha \frac{L}{2} \simeq \frac{L}{2}\frac{\omega}{v} = (2K+1)\frac{\pi}{2}) \tag{66}$$

with K integer number. The resonances frequencies are

$$\omega_k = (2K+1)\frac{\pi v}{L} = (2K+1)\omega_o \tag{67}$$

We obtain the result which we could have expected from general considerations on the tensorial character of GW that the resonance frequencies are only the odd modes (first, third...). As matter of fact it has been suggested that an oscillation on the second harmonic might be taken as indicative that the signal is due to noise or, more optimistically, that the GW do not have tensorial character.

For large values of Q and in proximity of a resonance, say ω_o, the solution 63 can be approximated with

$$\xi(\omega, z) \simeq h(\omega)\frac{L\omega_o sin\alpha z}{(\omega - \omega_o - \frac{i\omega_o}{2Q})\pi^2} \tag{68}$$

which is equal to that for a simple harmonic oscillator if we put

$$l = \frac{4L}{\pi^2} sin\alpha z \simeq \frac{4L}{\pi^2} sin\pi\frac{\omega}{\omega_o}\frac{z}{L} \tag{69}$$

This allows to use the simple solutions found for the simple oscillator by substituting the expression 69 for the length l.

6 The cross-section

We want to calculate the amount of energy absorbed by a resonant detector when interacts with a GW. We consider the case of a GW modelled with a delta-function.

Combining eqs. 50, 69 we find the displacement of a mass element at coordinate z

$$\xi(z,t) = -\xi_o e^{-\beta_1 t} sin\omega_o t sin\pi \frac{\omega}{\omega_o}\frac{z}{L} \tag{70}$$

where

$$\xi_o = \frac{2L}{\pi^2} h(\omega_o)\omega_o \tag{71}$$

Integrating over the bar length and in a time period we find the absorbed energy

$$E = \frac{1}{4} M\omega_o^2 \xi_o^2 \tag{72}$$

For calculating the energy carried by the GW we recall [1] that in general this energy per unit time and per unit surface is

$$I(t) = \frac{c^3}{16\pi G}(\dot{h}_+^2 + \dot{h}_\times^2) \tag{73}$$

For one polarization the total energy per unit surface is

$$I_o = \frac{c^3}{16\pi G}\int_{-\infty}^{\infty} \dot{h}(t)^2 dt \tag{74}$$

Using the Parseval identity we get

$$I_o = \frac{c^3}{16\pi G}\int_{-\infty}^{\infty} \omega^2 |h(\omega)|^2 df \tag{75}$$

where $f = \frac{\omega}{2\pi}$. The integrand is called *spectral density*. At the resonance

$$\Phi(f_o) = \frac{c^3}{16\pi G}\omega_o^2 |h(\omega_o)|^2 \qquad \frac{joule}{m^2 Hz} \tag{76}$$

The cross-section is defined by

$$\Sigma_o = \frac{E}{\Phi(f_o)} = \frac{16}{\pi}\frac{G}{c}(\frac{v}{c})^2 M \qquad m^2 Hz \tag{77}$$

This cross-section has been obtained using a two-side spectral density. For one-side spectral density we get one half of that given in eq. 77, as most often given in the literature.

The subscript o in Σ_o indicates that this cross-section has been obtained for the case of a GW impinging perpendicularly to the bar axis (see eq. 50). In the general case it can be shown [3] that the cross section is

$$\Sigma = \Sigma_o cos^4\theta cos^2 2\phi \tag{78}$$

where θ indicates the angle between the bar axis and the direction of the incoming wave and ϕ is the angle between the y-axis in the reference system where the bar axis coincide with the z-axis and the y_p-axis of the reference system where the eqs.7, 8 are valid.

The same result can be obtained [4, 5] on a more general basis, following the lines used in particle physics for determining the cross section of (for example) the neutron scattering.

A much larger cross-section is instead obtained following the Preparata [6] quantum theory of matter.

7 Interaction of a resonant detector with particles

The energy delivered by energetic particles to a body is much larger than that typical of a Brownian motion. For instance a high-energy muon can deliver an energy of the order of 200 MeV. In kelvin units this is $2\ 10^{12}\ K$. Fortunately, we are interested in the energy captured at the resonance, which is much less. We give here a very simple, almost naive, calculation of this energy [7].

When an energy E is dissipated in the resonant detector of mass M the temperature T increases by the amount

$$\triangle T = \frac{E}{cM} \tag{79}$$

where c is the specific heat.

Consequently the length L increases

$$\triangle L = \alpha L \triangle T \tag{80}$$

where α is the linear coefficient.

The largest energy of the vibration at the resonance frequency ω is

$$\epsilon = \frac{1}{4} M\omega^2 (\triangle L)^2 = \frac{1}{4}\omega^2 \frac{\alpha^2 L^2 E^2}{Mc^2} \tag{81}$$

The energy E delivered by the particle to the bar over a path l is

$$E = \frac{dE}{dx} l \tag{82}$$

Introducing the *Grüneisen* γ factor defined as

$$\gamma = 2v^2 \frac{\alpha}{c} \tag{83}$$

which is nearly constant over a large range of temperatures we get

$$\epsilon \sim \frac{1}{4}\omega^2 (\frac{\gamma}{2v^2})^2 \frac{L^4 (\frac{dE}{dx})^2}{\rho L^3} \tag{84}$$

where ρ is the metal density.

Roughly we get

$$\epsilon \sim \frac{1}{4}\omega^2 (\frac{\gamma}{2v^2})^2 \frac{E^2}{\rho} \sim 6\ 10^{-9} E^2 \tag{85}$$

where in the last equality we have expressed E in GeV unit and ϵ in kelvin unit.

More accurate calculations made by several authors [8, 9, 10] give approximately the same result, expressed by

$$\epsilon = 8\ 10^{-9} E^2 f \qquad\qquad kelvin \tag{86}$$

where f is a geometric factor.

8 Sensitivity and bandwidth of resonant detectors

The detectors of gravitational waves (GW) now operating [11, 12, 13, 14, 15] use resonant transducers (and therefore there are two resonance modes

coupled to the gravitational field) in order to obtain high coupling and high Q.

But for the discussion on the detectors sensitivity and frequency bandwidth it is sufficient to consider the simplest resonant antenna, a cylinder of high Q material, strongly coupled to a non resonant transducer followed by a very low noise electronic amplifier. The equation for the end bar displacement ξ is (see eq. 40)

$$\ddot{\xi} + 2\beta_1\dot{\xi} + \omega_o^2\xi = \frac{f}{m} \tag{87}$$

where f is the applied force, m the oscillator reduced mass (for a cylinder $m = \frac{M}{2}$) and $\beta_1 = \frac{\omega_o}{2Q}$ is the inverse of the decay time of an oscillation due to a delta excitation.

We consider here only the noise which can be easily modeled, the sum of two terms: the thermal (Brownian) noise and the electronic noise [16]. The power spectrum due to the thermal noise is

$$S_f = \frac{2\omega_o}{Q} mkT_e \tag{88}$$

where T_e is the equivalent temperature which includes the effect of the back-action from the electronic amplifier.

By referring the noise to the displacement of the bar ends, we obtain the power spectrum of the displacement due to the Brownian noise:

$$S_\xi^B = \frac{S_f}{m^2} \frac{1}{(\omega^2 - \omega_o^2)^2 + \frac{\omega^2\omega_o^2}{Q^2}} \tag{89}$$

From this we can calculate the mean square displacement

$$\bar{\xi^2} = \frac{kT_e}{m\omega_o^2} \tag{90}$$

that can be also obtained, as well known, from the equipartition of the energy.

To this noise we must add the wide-band noise due to the electronic amplifier (the contribution to the narrow-band noise due to the amplifier has been already included in T_e).

For sake of simplicity we consider an electromechanical transducer that converts the vibration of the detector in a voltage signal

$$V = \alpha\xi \tag{91}$$

with transducer constant α (typically of the order of 10^7 V/m). Thus the electronic wide-band power spectrum, S_o , is expressed in units of $\frac{V^2}{Hz}$ and the overall noise power spectrum referred to the bar end is given by

$$S_\xi^n = \frac{2kT_e\omega_o}{mQ}\frac{1}{(\omega^2-\omega_o^2)^2+\frac{\omega^2\omega_o^2}{Q^2}} + \frac{S_o}{\alpha^2} \tag{92}$$

We calculate now the signal due to a gravitational wave with amplitude h and optimum polarization impinging perpendicularly to the bar axis. The bar displacement corresponds [2] (see also eq. 69) to the action of a force

$$f = \frac{2}{\pi^2}mL\ddot{h} \tag{93}$$

The bar end spectral displacement due to a flat spectrum of GW (as for a delta-excitation) is similar to that due to the action of the Brownian force. Therefore, if only the Brownian noise were present, we would have a nearly infinite bandwidth [2], in terms of signal to noise ratio (SNR). For a GW excitation with power spectrum $S_h(\omega)$, the spectrum of the corresponding bar end displacement is

$$S_\xi = \frac{4L^2\omega^4 S_h}{\pi^4}\frac{1}{(\omega^2-\omega_o^2)^2+\frac{\omega^2\omega_o^2}{Q^2}} \tag{94}$$

We can then write the SNR

$$SNR = \frac{S_\xi}{S_\xi^n} = \frac{4L^2\omega^4 S_h}{\pi^4\frac{S_f}{m^2}}\frac{1}{1+\Gamma(Q^2(1-\frac{\omega^2}{\omega_o^2})^2+\frac{\omega^2}{\omega_o^2})} \tag{95}$$

where the quantity Γ is defined by [17]

$$\Gamma = \frac{S_o\beta_1}{\alpha^2\bar{\xi}^2} \sim \frac{T_n}{\beta Q T_e} \tag{96}$$

T_n is the noise temperature of the electronic amplifier and β indicates the fraction of energy which is transferred from the bar to the transducer. It can be readily seen that $\Gamma << 1$.

[2] Already several years ago Joe Weber pointed out this feature of an oscillator with a very low noise amplifier.

The GW spectrum that can be detected with SNR=1 is:

$$S_h(\omega) = \pi^2 \frac{kT_e}{MQv^2} \frac{\omega_o^3}{\omega^3} \frac{1}{\omega} (1 + \Gamma(Q^2(1 - \frac{\omega^2}{\omega_o^2})^2 + \frac{\omega^2}{\omega_o^2}) \tag{97}$$

where v is the sound velocity in the bar material (v=5400 m/s in aluminum). For $\omega = \omega_o$ we obtain the highest sensitivity

$$S_h(\omega_o) = \pi^2 \frac{kT_e}{MQv^2} \frac{1}{\omega_0} \tag{98}$$

having considered $\Gamma << 1$.

Another useful quantity often used is the *spectral amplitude*

$$\tilde{h} = \sqrt{S_h} \tag{99}$$

We remark that the best spectral sensitivity, obtained at the resonance frequency of the detector, only depends, according to eq.98, on the temperature T, on the mass M and on the quality factor Q of the detector, provided $T = T_e$. Note that this condition is rather different from that required for optimum pulse sensitivity (see later). The bandwidth of the detector is found by imposing that $S_h(\omega)$ be equal to twice the value $S_h(\omega_o)$. We obtain , in terms of the frequency $f = \frac{\omega}{2\pi}$

$$\triangle f = \frac{f_o}{Q} \frac{1}{\sqrt{\Gamma}} \tag{100}$$

The present detector bandwidths are of the order of 1 Hz, but it is expected that the bandwidths will become of the order of 50 Hz, by improving the amplifier noise temperature T_n , the coupling parameter β and the quality factor Q.

In fig.1 we show the spectral amplitude $\tilde{h}$ for the present Aluminium resonant detectors with mass M=2270 kg operating at a temperature T=0.1 kelvin and the target $\tilde{h}$ which will be reached with improved transducers. The parameters used for calculating the spectral amplitudes are given in table 1.

From eqs. 98 and 100 one can derive the antenna sensitivity to various types of GW. For delta-like bursts with duration τ_g the sensitivity is given by

$$h \simeq \frac{1}{\tau_g} \sqrt{\frac{2S_h}{\pi \delta f}} \tag{101}$$

Table 1: Bandwith and sensitivity for presently operating detectors and for future detectors with improved transducers.

T $[K]$	Γ	Q	$\triangle f$ $[Hz]$	$\tilde{h}_{min}$ $[\frac{1}{\sqrt{Hz}}]$
0.1	10^{-6}	$8.5\ 10^5$	1.1	$5.3\ 10^{-22}$
0.1	10^{-11}	$4.2\ 10^6$	70	$2.3\ 10^{-22}$

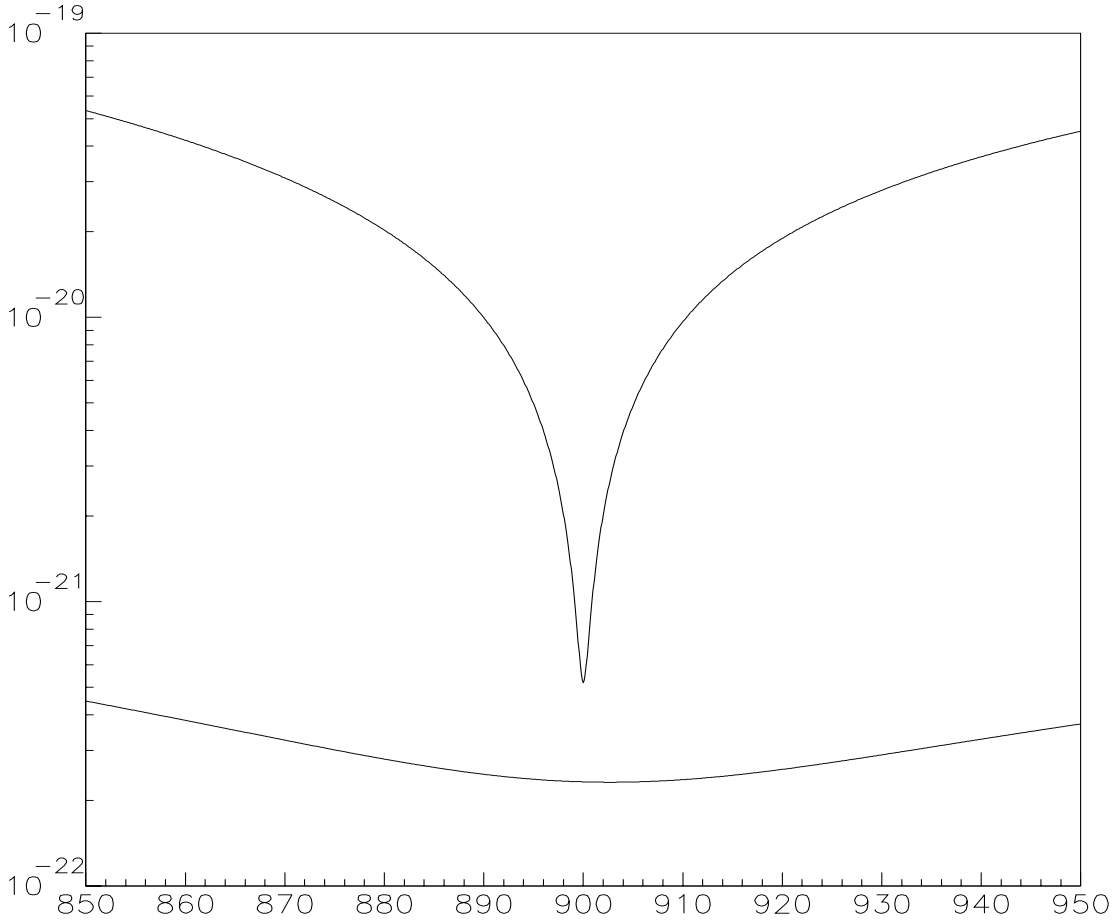

Figure 1: Spectral amplitudes $\tilde{h}$ present and planned, see eqs. 99 and 97, with parameters given in table 1 versus frequency $[Hz]$. The presently operating detectors have bandwidth $\sim$ 1 Hz. The bandwidth will be much larger in a near future with improved transducers.

Another useful formula (derived from eqs.98 and 100) is

$$h \simeq \frac{L}{\tau_g v^2}\sqrt{\frac{kT_{eff}}{M}} \tag{102}$$

where L is the length of the bar and T_{eff} is the noise temperature for burst detection, that is the average value of the noise after applying to the GW data a filter matched to delta-like signals.

For monochromatic GW the minimum wave amplitude that can be detected with SNR=1, integrating over a continuous time t_m, is

$$h = \sqrt{\frac{2S_h}{t_m}} \tag{103}$$

Finally eq.88 gives immediately the sensitivity to a GW stochastic background measuring an upper limit only, since it is practically impossible to subtract from the measured power spectrum the contribution due to noise.

In order to measure the stochastic background one needs to cross-correlate the output of two antennas [18] obtaining the measurement of the cross-spectrum

$$S_h(f) = \frac{\sqrt{S_{1h}S_{2h}}}{\sqrt{t_m \delta f}} \tag{104}$$

where t_m is the total time of crosscorrelation and δf is the frequency bandwidth in common between the two detectors. From the measured S_h we can calculate [18] the value of Ω, the ratio between the GW energy density and the energy density needed for a close Universe, using the formula

$$\Omega = \frac{4\pi^2}{3}\frac{f^3}{H^2}S_h(f) \tag{105}$$

where H is the Hubble constant. We notice that, while for burst detection it is important to have a large frequency bandwidth (attainable with a good transducer followed by a very low noise electronic amplifier), this is less important for the stochastic measurements.

9 Linear filtering for detection of GW short bursts

We treat this problem in the simple case of a resonant bar equipped with a non-resonant transducer (i.e., a piezoelectric ceramic) followed by a low noise amplifier. It is easy to generalize this procedure to the case of a resonant transducer.

The signal from the low noise amplifier is send to a lock-in amplifier which extracts the in phase and in quadrature components, $x(t)$ and $y(t)$, of the Fourier transform at the bar resonance frequency f_o. The lock-in amplifier has integration time t_o and both components are sampled with a sampling time $\triangle t = 1/t_o$, in order to minimize the amount of data to be recorded. The simplest algorithm for extracting a signal due to a GW short bursts from the noise, employed for the first time by Levine and Garwin and called in the Rome group the ZOP algorithm (zero-order prediction), consists in taking the difference between two successive samplings

$$z(t)^2 = [x(t) - x(t - \triangle t)]^2 - [y(t) - y(t - \triangle t)]^2 \tag{106}$$

The key idea is that a short burst will produce a jump in the data, like a hammer hit, while the fluctuations due to the noise have a relative long time constant. Let us now estimate the SNR for this algorithm. The noise is basically due to the narrow-band Brownian noise (in units of $volt^2$) in the bar

$$V_{nb}^2 = \alpha^2 S_f(f_o)\beta_1 \tag{107}$$

(increased by the back action from the amplifier) and to the white noise S_o from the amplifier. The auto correlation for this noise process at the lock-in output is

$$R(\tau) = V_{nb}^2[\frac{e^{-\tau/\tau_v} - \frac{t_o}{\tau_v}e^{-\tau/t_o}}{1 - t_o^2/\tau_v^2}] + \frac{S_o}{t_o}e^{-\tau/t_v} \tag{108}$$

for each components, $x(t)$ and $y(t)$, of the signal, where $\tau_v = \frac{1}{\beta_1}$ is related to the merit factor $Q = \tau_v \pi f_o$. From the above autocorrelation we derive the variance for the variable $z(t)$:

$$\sigma^2 = 4[R(0) - R(\triangle t)] = \frac{4V_{nb}^2}{e}\frac{\triangle t}{\tau_v} + 4\frac{e-1}{e}\frac{S_o}{\triangle t} \tag{109}$$

where we notice that there are two noises in competition, one increasing linearly with $\triangle t$ and the other one with the inverse of $\triangle t$. The optimum $\triangle t$ is given by

$$\triangle t_{opt} = \tau_v \sqrt{(e-1)\Gamma} \tag{110}$$

and

$$\sigma^2_{opt} = 8V^2_{nb} \frac{\sqrt{(e-1)\Gamma}}{e} \tag{111}$$

where we have made use of the quantity (see eq.(16))

$$\Gamma = \frac{S_o \tau_v}{V^2_{nb}} \tag{112}$$

We have now to calculate the signal for this algorithm. An incoming GW short burst will produce at the low noise amplifier output a jump in the signal from the noise level to a value

$$V_s = \alpha \frac{2L}{\pi^2} \omega_o h(\omega_o) \tag{113}$$

slowly decaying with the time constant τ_v. At the lock-in amplifier output (after the lock-in integration with time constant t_o) we take the difference between two next samples. If we assume that the signal arrives exactly at the time of a sampling the difference with the next sampling will give $V_s(1-1/e)$. We introduce the signal energy

$$E_s = \frac{1}{2} m \omega^2_o (\frac{V_s}{\alpha})^2 \tag{114}$$

Recalling that $V^2_{nb} = \frac{\alpha^2 k T_e}{m \omega^2_o}$, we get

$$SNR = \frac{V^2_s (1-1/e)^2}{\sigma^2_{opt}} = \frac{E_s}{4kT_e \sqrt{\Gamma}} \frac{1}{1.21} \tag{115}$$

It must be remarked that this results is valid for signals arriving exactly at the sampling times. If one considers signals arriving at random times he gets a SNR that, on the average, is smaller by several per cent.

The ZOP filter can be extended by including not just two samplings but many more. This is done by using the Wiener filter [16] that is based on

the idea that the data samplings are processed a few seconds after they have been recorded, in such a way to make use of past as well $future$ data. The measured variables $x(t)$ and $y(t)$ include signal and noise. The best estimation $u(t)$ of the signal for the variable $x(t)$ is

$$\tilde{u}(t) = \int x(t-\tau)W(t)d\tau \tag{116}$$

where $W(t)$ is the filter function which will be estimated with the linear mean square method. It can be demonstrated [16] that the Fourier transform $W(f)$ of $W(t)$ which minimize the average difference $< (u(t) - (\tilde{u}(t) >^2$ is

$$W(f) = \frac{S_{ux}(f)}{S_{xx}(f)} \tag{117}$$

where $S_{xx}(f)$ is the power spectrum of $x(t)$, and $S_{ux}(f)$ is the cross spectrum of $u(t)$ and $x(t)$.

The power spectrum of the brownian noise reported at the antenna input (in units of $\frac{V^2}{Hz}$) is white, $S_{uu} = \frac{2V_{nb}^2}{\beta_1}$ and so is white the noise $S_{ee} = 2S_o$ at the lock-in output, due to the electronic amplifier that enters in the electronic chain before the lock-in. We notice that $\Gamma = \frac{S_{ee}}{S_{uu}}$. We can then consider the overall electronic chain as made by two pieces. The first piece with transfer function $W_a(f)$ is the bar which, together with the selective part of the lock-in, acts as a low-pass filter with time constant τ_v, the second piece is the integrating part of the lock-in which is again a low-pass filter with transfer function W_e and time constant t_o. We get

$$S_{xx}(f) = S_{uu}W_a^2W_e^2 + S_{ee}\,W_e^2 \tag{118}$$

$$S_{ux}(f) = S_{uu}W_a^*W_e^* \tag{119}$$

from which we obtain

$$W(f) = \frac{1}{W_aW_e}\frac{1}{1+\frac{\Gamma}{W_a^2}} \tag{120}$$

which solves the problem. If one wants to apply the Wiener filter in the time-domain, he can calculate the coefficients $a_k = \int W(t)dt$ over several sampling intervals, $(k-1/2)\triangle t$ to $(k+1/2)\triangle t$, and the estimate

$$\tilde{u}_i \simeq \sum x_{i-k}a_k \tag{121}$$

Applying this filter to the data we get the power spectrum of the noise after the Wiener filter

$$S_{\tilde{u}\tilde{u}}(f) = S_{xx}W(f)^2 = \frac{S_{uu}}{1 + \frac{\Gamma}{W_a}^2} \tag{122}$$

From this we get the autocorrelation of the noise

$$R_{\tilde{u}\tilde{u}} = \frac{S_{uu}}{2\tau_v\sqrt{\Gamma(\Gamma+1}}e^{-\beta_3 t} \tag{123}$$

with

$$\beta_3 = \frac{1}{\tau_v\sqrt{(\Gamma+1)\Gamma}} \simeq \frac{1}{\tau_v\sqrt{\Gamma}} \tag{124}$$

Recalling eq.(23) we find that β_3 is the antenna bandwidth.

The signal reported at the antenna input has Fourier transform V_s (white spectrum because we consider a GW short burst). For simplicity, we consider the signal in phase with the lock-in reference frequency. The application of the Wiener filter gives

$$u(f) = V_s W_a(f) W_e(f) W(f) = \frac{V_s}{1 + \frac{\Gamma}{W_a}^2} \tag{125}$$

formally identical to eq.(14). We notice that in absence of electronics noise ($\Gamma = 0$) the estimation is perfect, in the sense that its Fourier transform is equal to the Fourier transform of the GW signal. From the above equations we get the maximum SNR at time $t = 0$, when the GW burst arrives, considering that there is an equal contribution to the noise both from the in-phase and from the in-quadrature responses of the lock-in,

$$SNR = \frac{u^2(t=0)}{2 \cdot R_{\tilde{u}\tilde{u}}(t=0)} = \frac{V_s^2}{2\tau_v S_{uu}\sqrt{\Gamma(\Gamma+1)}} = \frac{E_s}{4kT_e\sqrt{\Gamma}} \tag{126}$$

This shows that the improvement over the optimum ZOP filter seems to be just a factor of 1.21. Actually, the advantage is that, for the Wiener filter, one can sample faster than the optimum sampling needed to optimize the ZOP filter. In this way there is no loss in SNR due to the random arrival time of the GW bursts.

10 Search for coincidences. Events and signals.

Since the beginning of the GW research, the major goal has been to detect coincident events in two antennas located at large distance one from each other. The events are extracted from the raw data by applying algorithms (optimum filters, see for instance [20, 21]) based on least square procedures under the hypothesis that the signal exciting the detector can be represented with a delta function. In this section we want to discuss the effect of the noise on the signal.

After an optimum filter has been applied to the raw data a threshold is applied. When the filtered data go above this threshold, the time behaviour is considered until the filtered data go again below the threshold for more than a given time. The maximum amplitude and its occurrence time define the *event*.

By the word *signal* we mean the response of the detector to an external excitation in absence of noise. It is then evident that an *event* is a combination of signal and noise. In the following we shall use SNR to indicate the ratio between the *signal* energy, which we denote with E_s and the noise T_{eff},

$$SNR = \frac{E_s}{T_{eff}} \tag{127}$$

We shall denote with SNR_t the threshold energy referred to the noise.

The effect of the noise on the signal has been discussed in [22, 12, 19] and it turns out to be larger that one could erroneously think. For example, for $SNR \sim SNR_t$, one could think that most of the signals would be detected. It turns out that the detection efficiency is of the order of 50%, as the noise might be in phase with the signal, pushing it even higher over the threshold or in counter-phase, pushing it below the threshold. This means that the detection efficiency for m^{pl} coincidences with m detectors, in this case is of the order of $\frac{1}{2^m}$.

The noise acts also in producing an *event time* different from the time the *signal* was applied. This influences the choice of the coincidence time window.

By using a simulation [23] we have determined the efficiency of the signal detection for the Rome detectors EXPLORER and NAUTILUS, as shown in

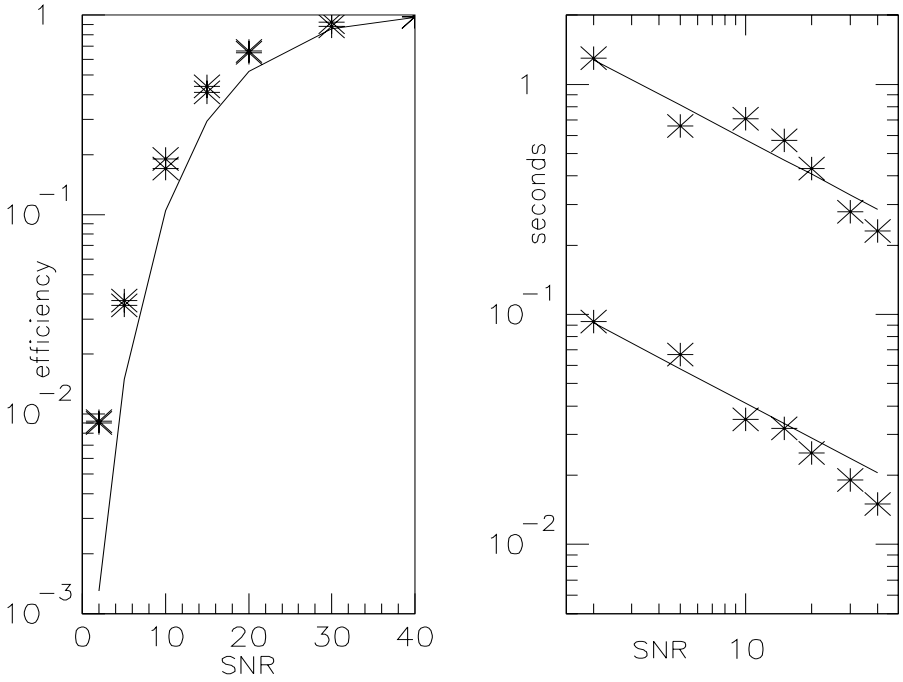

Figure 2: Threshold at $SNR_t = 19.5$. On the left figure the stars indicate the experimental efficiency for EXPLORER and NAUTILUS versus SNR of the applied signals, calculated with signal simulation on the real noise. The continuous line shows the expected theoretical efficiency. The discrepancy is due to the non gaussian character of the noise. On the right figure the standard deviation of the event time with respect to the signal time is shown versus SNR. The upper curve refers to NAUTILUS (bandwidth $\Delta f = 0.12\ Hz$). The lower curve refers to EXPLORER ($\Delta f = 1.9\ Hz$). The lines are the best fits. See text.

fig. 2. We notice that an event might be detected even if the signal producing it is below the threshold, and that signals originally above threshold can be lost. Only if the signal is more than twice the threshold the detection efficiency is near unity.

The time when the event is observed deviates from the time the signal is applied. We show, also in fig. 2, the standard deviation against SNR for EXPLORER 1991 and for NAUTILUS 1998 which have different bandwidth.

The lines are the best fits with the following equation

$$\sigma = \frac{1}{2\pi\Delta f}\sqrt{\frac{2}{SNR}} \tag{128}$$

This shows the effect of the bandwidth on the time dispersion.

11 Statistical problems in the search of coincidences

The analysis in a coincidence search consists essentially in comparing the detected coincidences at zero time delay with the background, that is with coincidences occurring by chance. In order to measure the background due to the accidental coincidences, using a procedure adopted since the beginning of the gravitational wave experiments [24], one shift the time of occurrence of the events of one of the two detectors a number of times, say 1,000 times in steps of 2 s, from -1,000 s to +1,000 s. For each time shift one get a number of coincidences. If the time shift is zero one get the number n_c of *real* coincidences. The background is calculated from the average number of the n_{shift} accidental coincidences obtained from the one thousand time shifts

$$\bar{n} = \frac{\sum_1^{1000} n_{shift}}{1000} \tag{129}$$

With this experimental procedure for the evaluation of the background one circumvent the problems arising from a non stationary distribution of the events, provided one test properly the distribution of the shifted coincidences. We show an example of a delay hystogram in fig. 3(see reference [26]). It can be verified that the distribution of these accidental coincidences obeys the Poisson distribution.

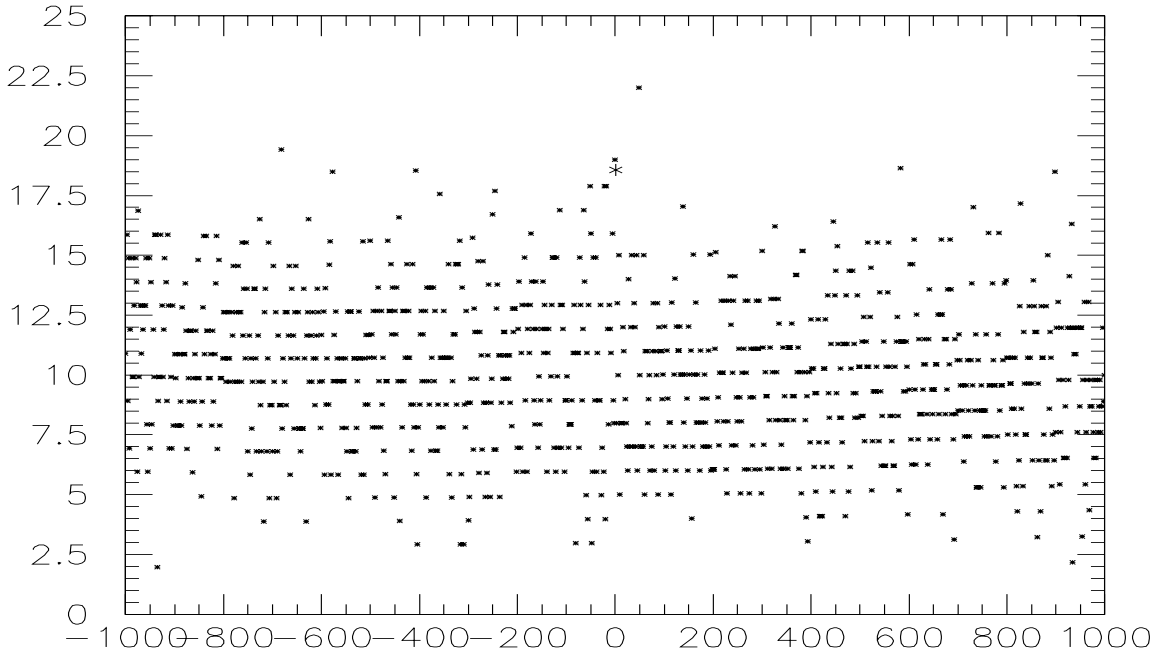

Figure 3: Example of a delay histogram for coincidences between EXPLORER and NAUTILUS. The biggest asterisk indicate $n_c = 19$ coincidences at zero time delay with a background $\bar{n} = 10.0$.

In comparing the number of coincidences n_c with the background one evaluate, using the Poisson formula, the probability P that the observed number n_c be due to a fluctuation of the background

$$P(\geq N) = 1 - \sum_{n=0}^{N-1} \frac{\bar{n}^n e^{-\bar{n}}}{n!} \tag{130}$$

If P turns out to be sufficiently small, one consider the possibility that the coincidence excess $\sim (n_c - \bar{n})$ be due, at least in part, to a signal or to non-gaussian noise. However one is faced with the possibility that the data producing the above result be only a subset of all possible data of that kind, perhaps, even unwillingly, selected by the experimenter in a way that favors the coincidence excess.

The only way to verify the correctness of a possible interpretation in terms of coincidence excess is to repeat the analysis using new data.

A more reliable approach is that provided by the Bayes theory. According to this theory the probability to have a certain result depends not only by the statistical computations on the experiment one is performing, but also by the degree of belief, due to previous information, to obtain that result.

To clarify this point we give the following example. Suppose we perform a coincidence experiment between two GW detectors. Suppose we obtain $n_c = 10$ coincidences while expecting by chance, on the average, $\bar{n} = 5$. We know the accidental coincidences have a Poissonian distribution. From eq. 130 we calculate the probability to have found $n_c = 10$ coincidences while expecting on average $\bar{n} = 5$. We get $P(n_c|\bar{n}) = 0.03$. This a rather small number (one would not bet against), yet we reasonably believe that is much more likely that the coincidence excess was not due to gravitational waves but to some other causes, other than a possible fluctuation of the background. We know this because gravitational wave have not been discovered yet, and extremely small signals are expected from the known theories.

If we want to express the result of our experiment by a probability (a probability we would bet in favor or against on equal grounds) we must write (following Bayes)

$$probability \equiv P_B(r|n_c, \bar{n}) = P(n_c|r, \bar{n})\ Prior(r) \tag{131}$$

where $Prior(r)$ express our belief to have r coincidences due to GWs. This

Prior depends only on previous information, and can be updated [1].

We want now to apply these considerations to the determination of upper limits. We introduce [27] the Bayes factor

$$R(r; n_c, \bar{n}) = \frac{f(n_c|r, \bar{n})}{f(n_c|r = 0, \bar{n})} \tag{132}$$

where r is the number of GW signals and $f(n_c|r, \bar{n})$ is the probability density and represents the likelihood that having measured $\bar{n}$ and having observed n_c coincidences we have r GW signals. R is called *relative belief updating ratio*.

Having considered the Poissonian distribution we have

$$f(n_c|r, \bar{n}) = \frac{e^{-(r+\bar{n})}(r + \bar{n})^{n_c}}{n_c!} \tag{133}$$

from which we obtain

$$R(r; n_c, \bar{n}) = e^{-r}(1 + \frac{r}{\bar{n}})^{n_c} \tag{134}$$

For clarifying the meaning of $R(r; n_c, \bar{n})$ we consider the example $\bar{n} = 5$ and $n_c = 10$. We want to estimate the upper limit for GW with given *bound*. Let us use eq. 134 and obtain fig. 4. The interpretation of this figure is the following:
Without considering the *Prior* one can say that the most likely case when $\bar{n} = 5$ and $n_c = 10$ is that there are five coincidences due to signals and five accidental coincidences. This is more likely that having a fluctuation of the background accounting for the ten coincidences (of course, our *Prior* nullifies this interpretation).

If we read the fig. 4 at the ordinate $r = 18$ we find $R(r; n_c, \bar{n}) = 0.05$. This means that the probability to have $r = 18$ GW signals is 5% of the probability that the observed number of ten coincidences be due to a background fluctuation. This result is independent on the assumed *Prior*. If we want to estimate the absolute probability to have $r = 18$, we must use eq. 132 introducing the *prior*. The final result turns out to be nearly independent on the *prior* in a wide range of choices, because no matter what we know from

[1] Of course the quantity $P_B(r|n_c, \bar{n})$ must vary between 0 and 1. This might need a normalizing constant.

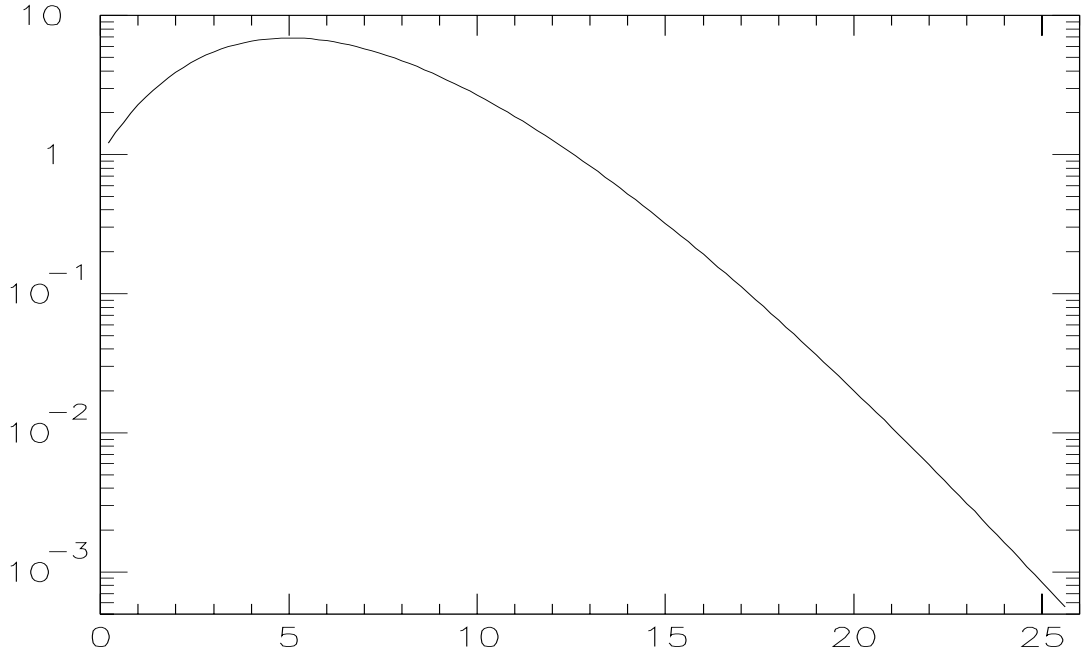

Figure 4: The *relative belief updating ratio* $R(r; n_c, \bar{n})$ versus the possible number r of GW signals, with $\bar{n} = 5$ and $n_c = 10$.

past information we certainly estimate improbable, with $\bar{n} = 5$ and $n_c = 10$, that we have $r = 18$ coincidences due to GW.

Consequently we infer that, assuming a uniform *prior*, $r = 18$ is the upper limit for the existence of GW signals, with a 5% degree of confidence.

12 Experimental results

After the initial controversial results by Weber [24]and an early null search for triple coincidences among Stanford, Louisiana and Rome [25] the following results have been obtained [3].

The most important problem with a detector is its calibration. A real calibration of a GW detector is not possible, since we do not dispose of a GW source, at present. But we can do alternative calibrations which can test the proper operation of the apparatus, even without checking whether it can really measure GW.

The Rome group has done it in two ways. At CERN with EXPLORER, the near gravitational field generated by a rotor in the vicinity of the detector has been measured [28]. The measurement was in very good agreement with the calculation made with the Newton law of gravitation.

In Frascati with NAUTILUS the signals produced by cosmic ray extensive air showers [29](EAS) were detected. This means that the apparatus is properly working and, in particular, the algorithms needed for extracting small signals from the noise are also very effective.

By averaging the effect of 92 EAS we found [30] the result shown in fig.5 in good agreement with the expectations, see eq. 86.

12.1 Upper limit

An upper limit for GW bursts has been determined [31] with the measurements made by ALLEGRO and EXPLORER in the year 1991. The upper limit is shown in fig. 6 where, in addition to the determination quoted in reference [31], a new determination applying the Bayesan statistics [32] is shown.

[3] We do not mention here the results obtained by the Rome group with a room-temperature bar during the SN1987A since, being an unique event, it requires a confirmation.

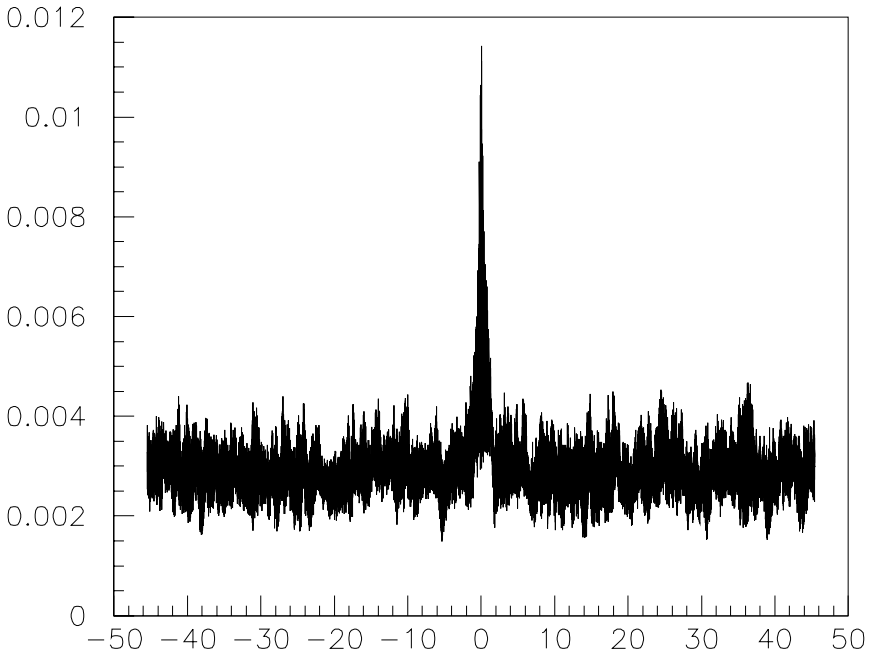

Figure 5: The average energy over 92 stretches of NAUTILUS data versus the time referred to the EAS arrival times.

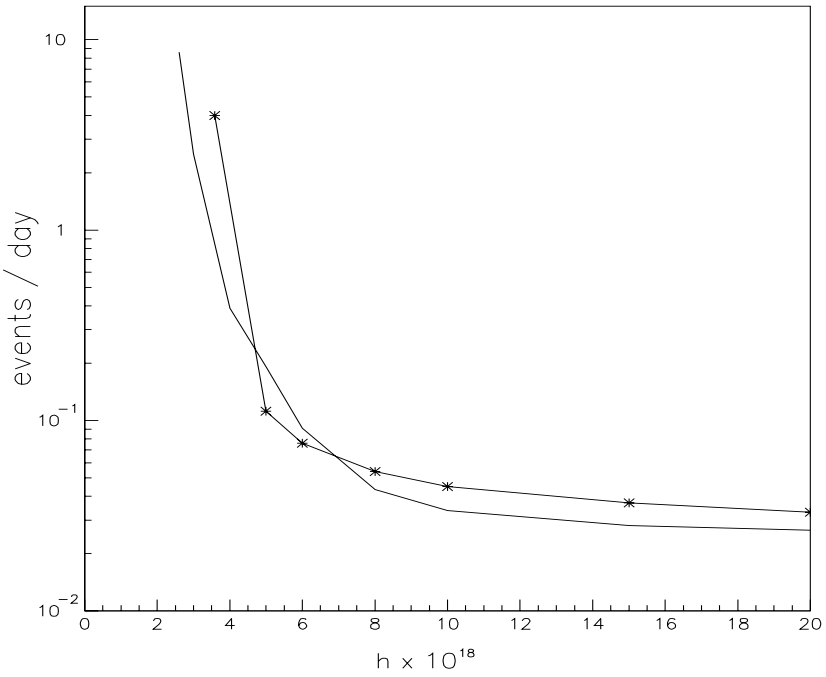

Figure 6: The asterisks indicate the upper limit calculated with the standard method. The line indicates the upper limit evaluated with the Bayesan approach.

12.2 Stochastic background

The crosscorrelation of the data taken with two detectors allows to measure the GW stochastic background. This has been done with the EXPLORER and NAUTILUS detectors [33] as illustrated in fig.7. The obtained value $\Omega = 60$ is much larger than the expected one, but this is the first measurement made with two cryogenic resonant GW detectors and it shows the feasibility of this type of experiment.

12.3 The IGEC collaboration

There are at present five cryogenic bars in operation [12, 15, 11, 14, 13] (Allegro, Auriga, Explorer, Nautilus and Niobe). They have roughly the same experimental sensitivity given in table 2. Niobe, made with niobium, has resonance frequency of 700 Hz, the other ones, with aluminum, have resonance

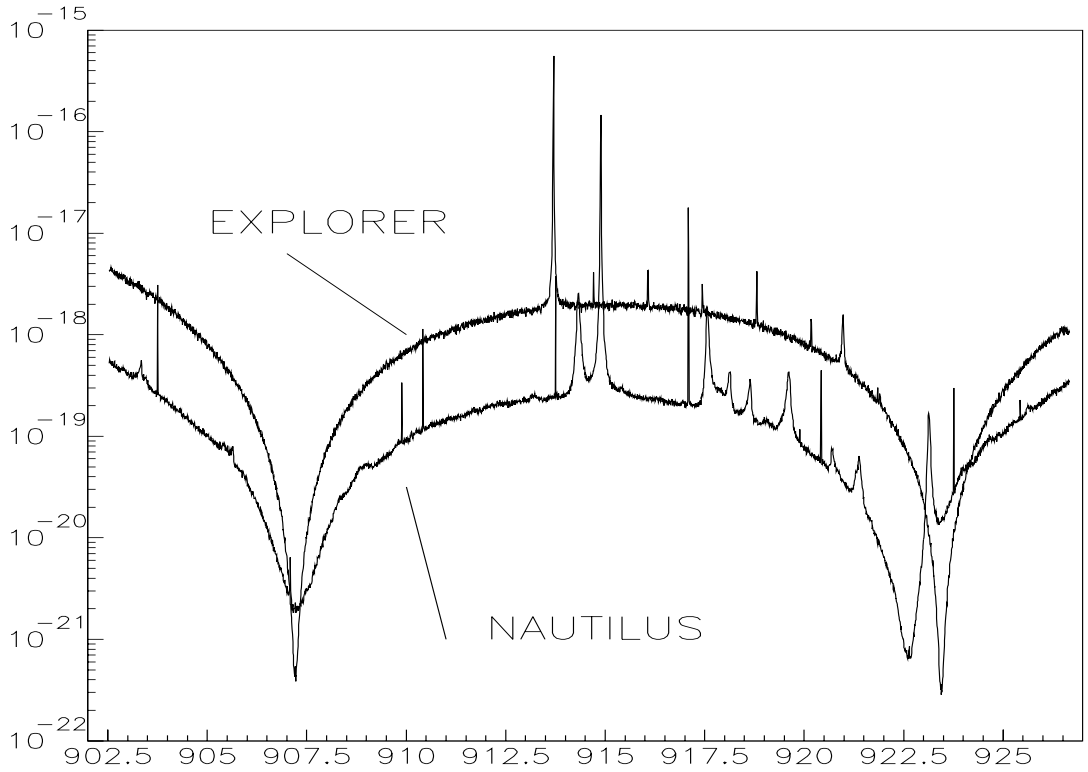

Figure 7: Spectral amplitude $\tilde{h}$ of EXPLORER and NAUTILUS versus frequency $[Hz]$.

Table 2: Sensitivity of the resonant detectors in operation

resonance frequency $[Hz]$	$\tilde{h} = \sqrt{S_h}$ at resonance $[\frac{1}{\sqrt{Hz}}]$	frequency bandwidth $\delta f\ [Hz]$	minimum h for 1 ms bursts	minimum h for continuous waves	minimum Ω
900-700	$7 \cdot 10^{-22}$	0.5-1	$4 \cdot 10^{-19}$	$2 \cdot 10^{-25}$	0.1

Table 3: IGEC collaboration. Net common observation time when at least N detectors were simultaneously operating.

N	days
1	625
2	260.4
3	89.7
4	15.5
5	0

frequency near 900 Hz. The above minimum values for monochromatic waves and for the quantity Ω have been estimated for one year of integration time (we suppose to use the cross-correlation of two identical antennas).

On July 1997 the IGEC (International Gravitational Event Collaboration) was established among the groups of
ALLEGRO, AURIGA, EXPLORER/NAUTILUS and NIOBE.
Each group has put on a common WEB site the list of the events extracted independently from the data of its own detector. The five detectors were in operation only part of the time. In table 3 we give the number of days during the years 1997 and 1998 when N detectors were simultaneously taking data. The coincidence search during this period gave no excess over the accidental coincidences [34]. However due to the short time period of observation there was no improvement on the previously determined [31] upper limit.

12.4 Coincidences among EXPLORER, Nautilus and NIOBE

Before the work within the IGEC Collaboration, coincidences were searched among the above three detectors. No double coincidence excess was found between EXPLORER and NIOBE and NAUTILUS and NIOBE, but some intriguing result was found when searching for coincidences between EXPLORER and NAUTILUS [35]. We show in Table 4 some result obtained when searching for coincidences between Explorer and Nautilus during the years 1995 and 1996.

In the first column we give the number of days when both antennas were simultaneously operating. The small number of useful days shows that it was

Table 4: Results of a coincidence search between data from Explorer and Nautilus during the years 1995 and 1996. See text for explanation.

number of days	number of Explorer events	number of Nautilus events	$\tilde{n}$	n_c	$p_{poisson}$ %
29.2	8527	5679	11.0	19	1.5

difficult to keep a cryogenic GW antenna in operation continuously with good behavior. At present a coverage of about 70% of the total time is attained. In the second and third column we show the number of *candidate events*. We notice the large number of candidate events that make practically impossible, on individual basis, to search for a particular signal due to GW. The big improvement is obtained by the comparison of the two detectors. Then we have to worry only for the number of accidental coincidences. In the fourth column we give the expected number of accidental coincidences measured by means of 10,000 shifts of the event times of one detector with respect to the other one. This number of accidentals is small enough to start considering the possibility to search for a coincidence excess (though, according astrophysical expectations, this excess should be much smaller than the observed number of accidentals). In this case the number of coincidences n_c, reported in column five, turns out to be slightly larger than the expected number of accidentals. Finally in columns sixth we report the Poisson probability that the observed excess was accidental.

13 Perspectives for resonant detectors

The burst sensitivity for all bars can be increased by improving the transducer and associated electronics. It has been estimated [36] that a factor of 50 be within the technical possibilities.

In addition to increase the bandwidth, Auriga and Nautilus can improve, see table 5, their spectral sensitivity by making full use of their capability to go down in temperature to $T = 0.10$ K. At present the major difficulty is due to excess noise, sometimes of unknown origin, and work is in progress for eliminating this noise.

New resonant detectors of different shape and much larger mass [37, 38, 39, 40] have been proposed for obtaining a greater sensitivity. The best

Table 5: Target sensitivity for Auriga, Nautilus and a spherical detector.

Detector	$\tilde{h} = \sqrt{S_h}$ at resonance $[\frac{1}{\sqrt{Hz}}]$	frequency bandwidth δf [Hz]	minimum h for 1 ms bursts	minimum h for continuous waves	minimum Ω
AURIGA NAUTILUS	$6 \cdot 10^{-23}$	50	$3 \cdot 10^{-21}$	$2 \cdot 10^{-26}$	10^{-4}
SPHERE 38 tonne	$6 \cdot 10^{-24}$	50	$3 \cdot 10^{-22}$	$2 \cdot 10^{-27}$	10^{-6}

geometry for a resonant detector is the spherical one, because a sphere has the largest possible mass for a given occupied space and because a spherical detector can be instrumented with transducers installed in various locations on its surface, allowing the best detection of GW with any direction and polarization.

Among various proposals an aluminum sphere with a diameter of 3 m, having the mass M=38 ton and operating at T=20 mK has been considered. The estimated sensitivity for this detector is shown in table 5. We have assumed that the detector operates near the quantum limit, that is with $T_{eff} \sim 10^{-7}$ K.

Furthermore we must consider that the sphere is sensitive to GW with any incoming direction and degree of polarization and is sensitive also to scalar GW.

14 Conclusions

Today there are sensitive resonant antennas in operation, producing data in an unexplored field of physics, allowing at least to obtain new upper limits for various types of GW.

It is important to realize that it is possible to increase the sensitivity of the resonant detectors by two orders of magnitude, approaching the limit for GW predicted by the present viable theories.

Finally we want to call the attention to the importance to develop spherical detectors, which are really complete GW observatories, for all directions, polarizations and able to discriminate among various possible theories of

gravity.

References

[1] L.D.Landau and E.M.Lifshitz "The classical theory of fields" Pergamon Press, Oxford (1971)

[2] G.Pizzella,Rivista del Nuovo Cimento 5,369 (1975)

[3] G.Pizzella "Fisica sperimentale del campo gravitazionale" La Nuova Italia Scientifica, Roma (1993)

[4] S.Weinberg "Gravitation and Cosmology" John Wiley and Sons, Inc. New Kork (1972)

[5] R.Ruffini and J.A.Wheeler "Relativistic cosmology and space platforms" Proc. of ESRO Colloquium, Interlaken (1969)

[6] G.Preparata Modern Physics Lett. A, 5 (1), 1-5, (1990)

[7] P.Michelson, private communication, 1982.

[8] A.M.Allega and N.Cabibbo Lett. Nuovo Cimento 38,263(1983)

[9] A.DeRujula and S.L.Glashow, Nature 312,734(1984)

[10] G.Liu and B.Barish, Phys.rev.lett 61,271(1988)

[11] P. Astone et al., Phys. Rev. D. 47, 362 (1993).

[12] E. Mauceli et al., Phys.Rev. D, 54, 1264 (1996)

[13] D.G. Blair et al., Phys. Rev. Lett. 74, 1908 (1995).

[14] P. Astone et al., Astroparticle Physics, 7 (1997) 231-243

[15] M.Cerdonio et al., First Edoardo Amaldi Conference on Gravitational wave Experiments, Frascati, 14-17 June 1994

[16] A.Papoulis "Probability, Rnadom variables and stochastic process" McGrow-Hill Book Co., New York (1965)

[17] G.V.Pallottino and G.Pizzella, in "Data Analysis in Astronomy III" pag.361, Ed. V. Di Gesu, L. Scarsi, P. Crane, J.H. Friedman, S.Levialdi, M.C.Maccarone, Plenum Press 1998.

[18] P.Astone, G.V.Pallottino, G.Pizzella, Class. Quantum Grav. 14 (1997) 2019-2030

[19] P.Astone, G.V.Pallottino, G.Pizzella, Journal of General Relativity and Gravitation , 30(1998)105-114

[20] P.Astone, P.Bonifazi, G.V.Pallottino, G.Pizzella, Il Nuovo Cimento 17,713 (1994)

[21] P.Astone et al., Il Nuovo Cimento 20,9,1997

[22] S.Boughn et al., Astrophys. J. 261, 119 (1982)

[23] P.Astone, S.D'Antonio and G.Pizzella, "Time dispersion and efficiency of detection for signals in GW experiments", January 2000, e-Print Archive: gr-qc/0001030 To appear on PRD (2000).

[24] J. Weber, Phys. Rev. Lett. 22, 1320 (1969).

[25] E.Amaldi et al. Astronomy and Astrophysics,vol216,pag 325-332,june 1989.

[26] Quarto

[27] P.Astone and G.D'Agostini, *"Inferring the intensity of Poisson processes at the limit of the detector sensitivity"*, CERN-EP/99-126

[28] P. Astone et al. Zeit. Script C - Particles and Fields, 50,21 (1991)

[29] E.Amaldi and G.Pizzella Il Nuovo Cimento 9,612 (1986)

[30] P.Astone et al., PRL,84,14 (2000)

[31] P.Astone et al. Phys.Rev. D, 59,122001, (1999)

[32] P.Astone and G.Pizzella, "On upper limits for gravitational radiation" January 2000, e-Print Archive: gr-qc/0001035

[33] P.Astone et al., Astron.Astrophys. 351,(1999)811-814

[34] G.A.Prodi, I.S.Heng et al. To be published in the proceedings of 4th Gravitational Wave Data Analysis Workshop (GWDAW 99), Rome, Italy, 2-4, Dec 1999. Submitted to Int.J.Mod.Phys.D e-Print Archive: astro-ph/0003106

[35] P.Astone et al., Astroparticle Physics 10 (1999)83-92

[36] M.Bassan and G.Pizzella, "Sensitivity of a capacitive transducer for resonant gravitational wave antennas", Internal Report, LNF-95/064, Frascati (1995)

[37] R.Forward, Journal of General Relativity and Gravitation 2, 199 (1971)

[38] W.W. Johnson and S.M. Merkowitz , Phys. Rev. Letters 70, 2367 (1993)

[39] E.Coccia, J.A. Lobo and J.A. Ortega, Phys. Rev. D 52, 3735 (1995)

[40] G. Frossati "A 100 ton 10 mK Gravitational Wave Antenna", Proceedings of the First Intern. Workshop OMNI 1, 26-31 May 1996, Sao Jose dos Campos (Brazil), World Scientific 1997.